Development of Procedures for Rapid Estimation of Ground Motions

Douglas S. Dreger, Asya Kaverina, Peter Lombard, Lind Gee and Douglas Neuhauser

University of California

Berkeley Seismological Laboratory

Pacific Earthquake Engineering Research Center

University of California, Berkeley

February 2002

Abstract

A new near-realtime software system that automatically determines the finite-source parameters of regionally-recorded earthquakes, and uses this information to estimate the level of near-fault strong shaking, has been developed and implemented as part of the Rapid Earthquake Data Integration (REDI) system at the Berkeley Seismological Laboratory (BSL). The method has been functionally integrated with the TriNet ShakeMap software [e.g. Wald et al., 1999]. This approach utilizes three-component regional distance broadband waveforms to resolve the fault plane orientation, fault dimensions, and rupture kinematics of earthquakes in near-realtime, which is then used to estimate the level of near-fault ground motions. The ground motion estimation involves several steps, including the use of directivity-corrected attenuation relationships and the direct integration of the fault slip distribution using near-source Green's functions. The estimated near-fault ground motion parameters are provided as input to the ShakeMap software to produce updated maps of strong ground shaking. The system is currently operating in a testing mode at the BSL, and efforts are underway toward the adoption of the method as a component of the authoritative ShakeMap system for the State of California.

Acknowledgements

We are grateful to the TriNet organizations for providing the data used in the development and testing of this system, and to David Wald for the ShakeMap V2.x software. We wish to acknowledge Jack Boatwright and Howard Bundock for their assistance with the ShakeMap V2.x code, and useful discussions on the application of ShakeMaps in Northern California. Figures were prepared using Generic Mapping Tools (GMT) [Wessel and Smith, 1991]. The method was conceived from research conducted under NEHRP contract 1434-HQ-GR-02742. The development and implementation of the system was supported by the PEER/Lifelines program under a PGE/PEER Phase II contract, PGE-009566.

"*This work was supported in part by the Pacific Earthquake Engineering Research Center through the Earthquake Engineering Research Centers Program of the National Science Foundation under Award number EEC-9701568*."

Table of Contents

Abstract…… iii
Acknowledgements……iv
Table of Contents……v
List of Figures……...v

1. **Introduction**……...1

2. **Automation of Finite Source Method**…..……..….3
   2.1 ***Method Overview***…….……...3
   2.2 ***Application***……...…8
3. **Analyst Review Tool**……..……..……..11
4. **Conclusions**……15
   4.1 ***Work Completed***……15
   4.2 ***Future Effort***…….15
5. **References**…..…….17
6. **Appendix**…….17
   6.1 ***Geophysical Research Letters Paper***……17
   6.2 ***Bulletin of the Seismological Society of America Paper***…….17

List of Figures

Fig. 2.1 Schematic diagram of realtime processing stream…...…..……...……4
Fig. 2.2 Summary of three levels of ShakeMap.....……...…7
Fig. 2.3 Hector Mine Application…….9
Fig. 2.4 Comparison of preliminary and revised Shake Maps for Hector Mine….10
Fig. 3.1 Screen shot of the analyst interface……...12
Fig. 3.2 Example of analyst interface for Portola earthquake……13

1. Introduction

Maps of strong ground motion parameters such as peak ground acceleration (PGA), peak ground velocity (PGV) and spectral acceleration (Sa) at discrete periods provided in near-realtime are considered by emergency responders to obtain an overview of the earthquake emergency, make decisions on deploying resources, and to facilitate the recovery. This information is most useful in the first 30 minutes following an earthquake. The ShakeMap method developed by the TriNet project [Wald et al., 1999] calculates maps of PGA, PGV, Sa (at periods of 0.3 1.0 and 3.0 seconds), as well as instrumental intensity. The reported ground motions are based on observed time histories combined with estimates from suitable attenuation relationships. The results are most robust in areas with a dense distribution of strong motion stations, such as in the major urban areas of the Los Angeles basin and the San Francisco Bay Area under the scope of the California Integrated Seismic Network (CISN). In many areas of California and the United States, the density of realtime reporting strong motion networks is insufficient to provide optimal results. For these areas, and to serve as a redundant approach in the well-instrumented regions, we have developed an earthquake source-physics-based approach. The method described below has been incorporated into the REDI system in operation at the BSL, and is currently operating in realtime on the test system. As configured, it is capable of determining finite-source information and near-fault strong shaking parameters for earthquakes in central and northern California. Although it is presently in a test mode, protocols for providing information (finite-fault and augmented ShakeMap) from this system to the Menlo Park office of the U.S. Geological Survey have been established. Additionally, we continue to work with the Northern California ShakeMap Working Group toward the adoption and integration of the procedures described here into the authoritative ShakeMap system for Northern California.

2. Automation of Finite-source Inversion

2.1 Method Overview

The Berkeley Seismological Laboratory (BSL) collaborates with the USGS at Menlo Park to operate the Joint Notification System (JNS), in which waveform and parametric data, and derived source information is exchanged and reported in realtime. The JNS provides earthquake location and magnitude information within 30 seconds to 4 minutes (depending on the level of the analysis) of the occurrence of an earthquake in central and northern California. For M>3.4 events broadband waveform data from the Berkeley Digital Seismic Network (BDSN) are requested and automated procedures for determining the seismic moment tensor are initiated [e.g. Pasyanos et al., 1996]. Currently the seismic moment tensor is determined within 6-9 minutes after the origin time of an event. In addition, strong motion data are processed to determine the PGA, PGV and Sa parameters for the earthquake, and provided to the ShakeMap systems operating in parallel at the USGS Menlo Park and BSL. At the BSL, for M_W>4.9 events, broadband and strong motion waveform data are requested, sent to a dedicated processing computer, and the automated finite-source/ShakeMap procedure is initiated. Figure 2.1 is a schematic of the near-realtime processing stream that has been developed. With this system a hierarche of ShakeMaps are produced. The first is available within several minutes of the event, and two updates that utilize finite-source information are available approximately 15 to 30 minutes after a given event.

A fundamental assumption of our method is that regional broadband data may be used to invert the seismic representation theorem (eqn 1) for the distribution of fault slip using appropriate regional distance Green's functions. Given the obtained finite-source model, near-fault time histories are simulated using the seismic representation theorm and appropriate near-fault Green's functions. The seismic representation is given in a simplified form below,

$$u_n(\vec{x},t) = \int_{-\infty}^{\infty} d\tau \iint_{\Sigma} \mu \hat{\eta}_i U_j(\vec{\xi},\tau) G_{ni,j}(\vec{x},\vec{\xi};t-\tau) d\Sigma \qquad (1)$$

u_n is the nth component of observed ground displacement. x and t are the spatial location of the station and time. On the right hand side U is the fault slip, which depends upon both

spatial position, ξ, on the fault, and time, τ. μ is the rigidity, and η is a unit vector defining the orienation of the fault plane. G is the Green's function that describes the impulse response of each point on the fault to each recording station. The indices n, i, j refer to geographical orientation. Given regional observations of ground displacement the fault slip is solved for in an inverse fashion following Hartzell and Heaton [1983]. Given the fault slip and near-fault Green's functions the forward calculation is performed to determine near-fault displacement time histories, which are used to determine PGA, PGV and Sa.

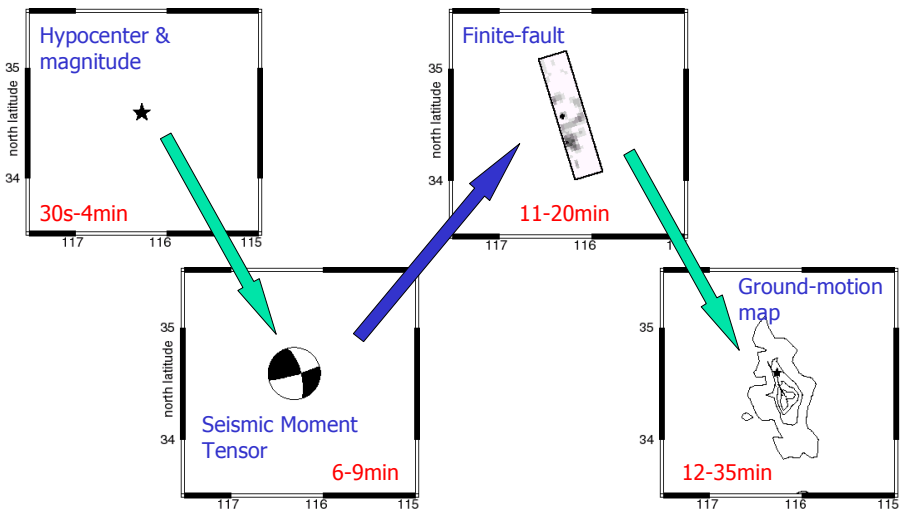

Fig 2.1 Schematic showing the general processing stream. The hypocenter and magnitude are determined from the JNS. The seismic moment tensor is determined within 6-9 minutes by the BSL REDI system. The finite-fault and ground-motion map boxes are components developed under this study. The times that the information is determined with respect to the event origin time are shown.

The first stage of the finite-fault processing involves solving for the best line-source solution. This is done by using the scaling relationships of Wells and Coppersmith [1994] and Somerville et al. [1999] to determine the dimension of the model fault plane. The dimensions derived from these relationships are doubled and then increased by an additional 10% safety factor to ensure that the model fault plane is large enough to account for unilateral rupture in either direction. The broadband displacement data are inverted using line-source models for both of the nodal plane orientations from the moment tensor results. The line-source inversions are

performed over a range of rupture velocity to find the optimal value. The dislocation rise time is held fixed and is determined *a priori* from the scalar seismic moment [e.g. Dreger and Kaverina, 2000; Somerville et al., 1999]. The line-source inversions are very fast, and result in a determination of the causative fault plane, the fault length, and the rupture velocity.

The second stage of the finite-fault processing involves the estimation of PGA, PGV and Sa using attenuation relationships corrected for directivity following the method of Somerville et al. [1997]. The ground motion estimates are then provided to the ShakeMap software, which combines the estimated and observed ground motions to produce an updated ShakeMap.

In the third stage, a planar-fault inversion is performed to determine the slip distribution of the event. The dislocation rise time as determined above and the best rupture velocity from the line-source inversions are assumed, and held constant. Only a single fault plane is used and the slip direction (rake) is also held fixed. This is a relatively simple parameterization, which is necessary to keep processing times short for emergency response applications. Offline analysis of the results can incorporate multiple fault segments, variable slip direction, and multiple time windows to account for dislocation rise time and rupture velocity variability as shown in the appendix. The finite-fault box in Figure 2.1 illustrates the mapview projection of the finite-fault results for the Hector Mine earthquake [e.g. Dreger and Kaverina, 2000]. The rectangle shows the surface projection of the fault plane model. The epicenter is shown as a star in the center of the rectangle, and the shades of gray represent the slip distribution. The slip distribution obtained in this way for Hector Mine is bilateral, however the largest slip is located to the southeast of the epicenter indicating a component of southward directivity.

The fourth stage of processing deterministically integrates the fault slip model using appropriate near-fault Green's functions to synthesize time histories. PGA, PGV and Sa are determined from the time histories, and combined with the values from the second stage by taking the larger of the two estimates. The estimated ground motion parameters are then provided to the ShakeMap software, which incorporates the observations and generates the ShakeMap. This final ShakeMap includes the effects of source finiteness, source directivity and the earthquake specific slip distribution in the estimates used to interpolate the data. For the earthquakes tested (1992 Landers, 1994 Northridge, and 1999 Hector Mine), in areas with very few strong motion recording instruments, the method produces a superior estimation of likely near-fault strong motion levels. The ground-motion box in Figure 2.1 illustrates the PGV map

obtained for the Hector Mine earthquake for the finite-source model shown. The contours of this map begin at 20 cm/s and are for intervals of 20 cm/s. The map clearly shows a pronounced southward directivity effect.

The actual ShakeMap processing involves the generation of three tiers of maps. The first is a TriNet ShakeMap [Wald et al., 1999], the second we call the Empirical ShakeMap, and the third we call the Conservative ShakeMap. An example of the program output, and description of the processing stream for each ShakeMap tier for a recent M6 earthquake in Mammoth Lakes, CA is provided in Figure 2.2. The top row of the flow chart shows the improvements in earthquake source information with increasing time from left to right. The TriNet ShakeMap utilizes event location, magnitude, observed ground motions, and point-source attenuation. The Empirical ShakeMap applies finite-fault/directivity corrections to the attenuation relationships [e.g. Somerville et al., 1999] and combines those estimates with the observations. The Conservative ShakeMap combines the larger of the estimated ground motions for the Empirical ShakeMap and deterministic ground motion estimates determined from the derived finite-fault slip model with the observations. For the TriNet ShakeMap the ground motion estimates are calculated internally. For the Empirical and Conservative ShakeMaps they are computed separately and provided to the ShakeMap V2.x software that combines the model estimates and observerations following the approach outlined in Wald et al. [1999]. The observation/estimate selection, interpolation of values, application of site corrections, and the contouring of each ShakeMap is performed by the ShakeMap V2.x software. The three maps are generated in the 4-6, ~15, and ~30 minute post-earthquake time frames, respectively.

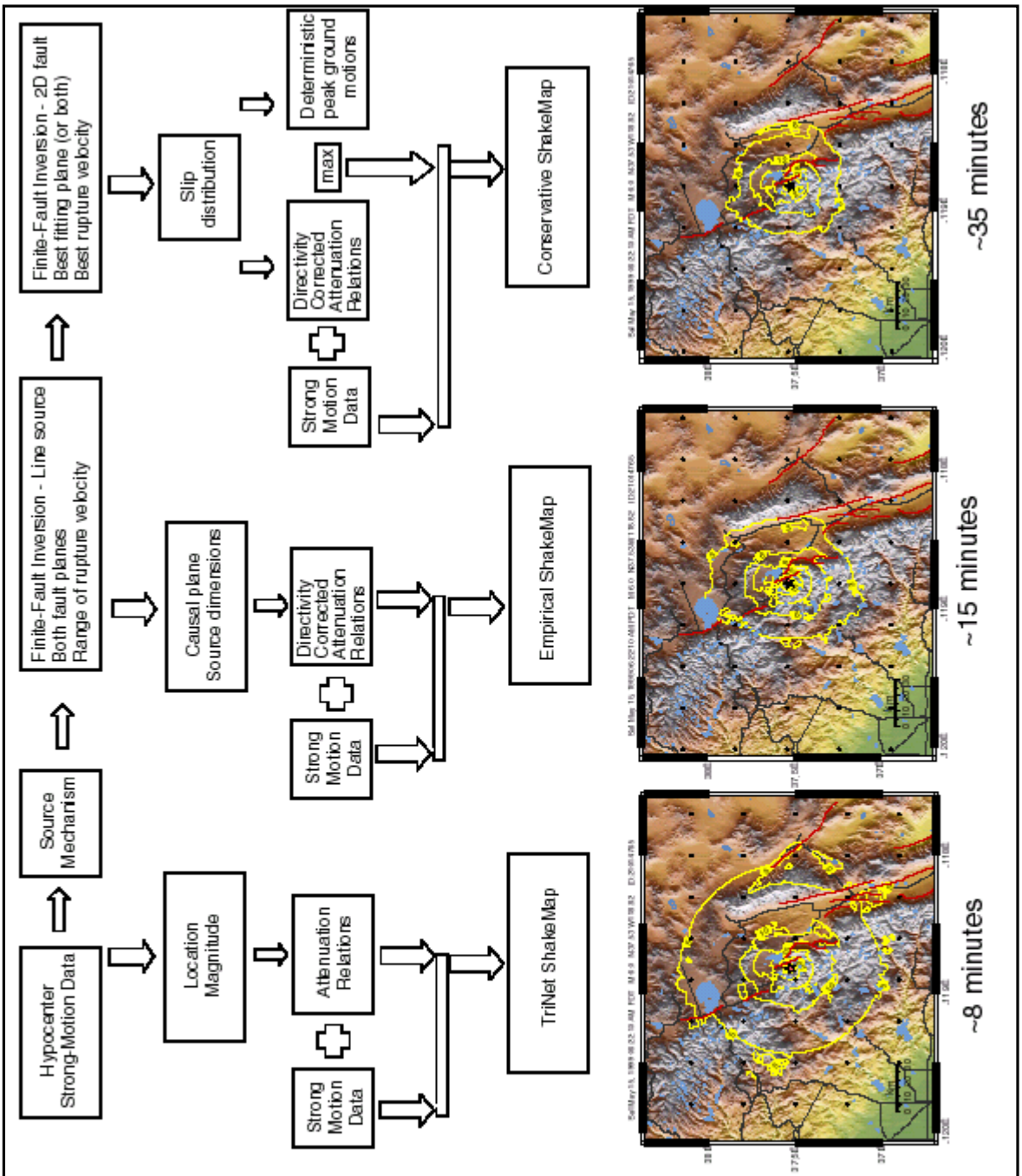

Figure 2.2. Summary of the three levels of ShakeMap produced by the REDI system, with an example of a M6 event in the Mammoth Lakes region. Note that the contour intervals vary from plot to plot. The time from the event origin when each map is produced is noted below each of the ShakeMaps.

2.2 Application

To validate the procedure we show the results for the October 16, 1999 Hector Mine earthquake as an example. Detailed discussion on our modeling of this event may be found in Dreger and Kaverina [2000], and Kaverina et al. [2002], which are also provided in the appendix. The Hector Mine earthquake (Mw7.1) was well recorded by the broadband stations of the Southern California networks (Figure 2.3a). As described above, we performed a series of eighteen line-source inversions for the two possible nodal planes from the event's moment tensor solution. As Figure 2.3b shows the data strongly prefer the north-south striking nodal plane with a rupture velocity of 2.6 km/s. Dreger and Kaverina [2000] discusses how the model dimensions of the line and plane source inversions and the assumed dislocation rise time are determined. Using the north-south striking plane and the derived rupture velocity the slip distribution shown in Figure 2.3c was obtained. The rectangle shows the surface projection of the fault model, and the hypocenter is labeled as a plus. The hypocenter is centered in the rather large fault model because we do not know *a priori* whether the rupture is bilateral or unilateral in either direction. In this preliminary model of Dreger and Kaverina [2000], it is shown that most of the slip is located to the south of the hypocenter suggesting a strong directivity effect. Solving the forward problem using the derived slip distribution, near-fault seismograms are computed to determine strong ground motion parameters such as PGA, PGV and Sa. Calculated PGV is compared to observed PGV (shown as numbers in units of cm/s) in Figure 2.3d. The three closest stations with the largest amplitudes were not available in the realtime epoch and were not used to determine the source parameters. The comparison shown in Figure 2.3d indicates that the estimated values for the near-fault region are reasonably good.

Subsequent analysis has shown that the Hector Mine earthquake was very complex involving multiple fault segments, and along strike variations in both rupture velocity and dislocation rise time [Kaverina et al., 2002; Ji et al., 2002]. In Kaverina et al. [2002] additional seismic, geodetic and surface faulting data were incorporated. A detailed description of this modeling and discussion of the results can be found in the appendix.

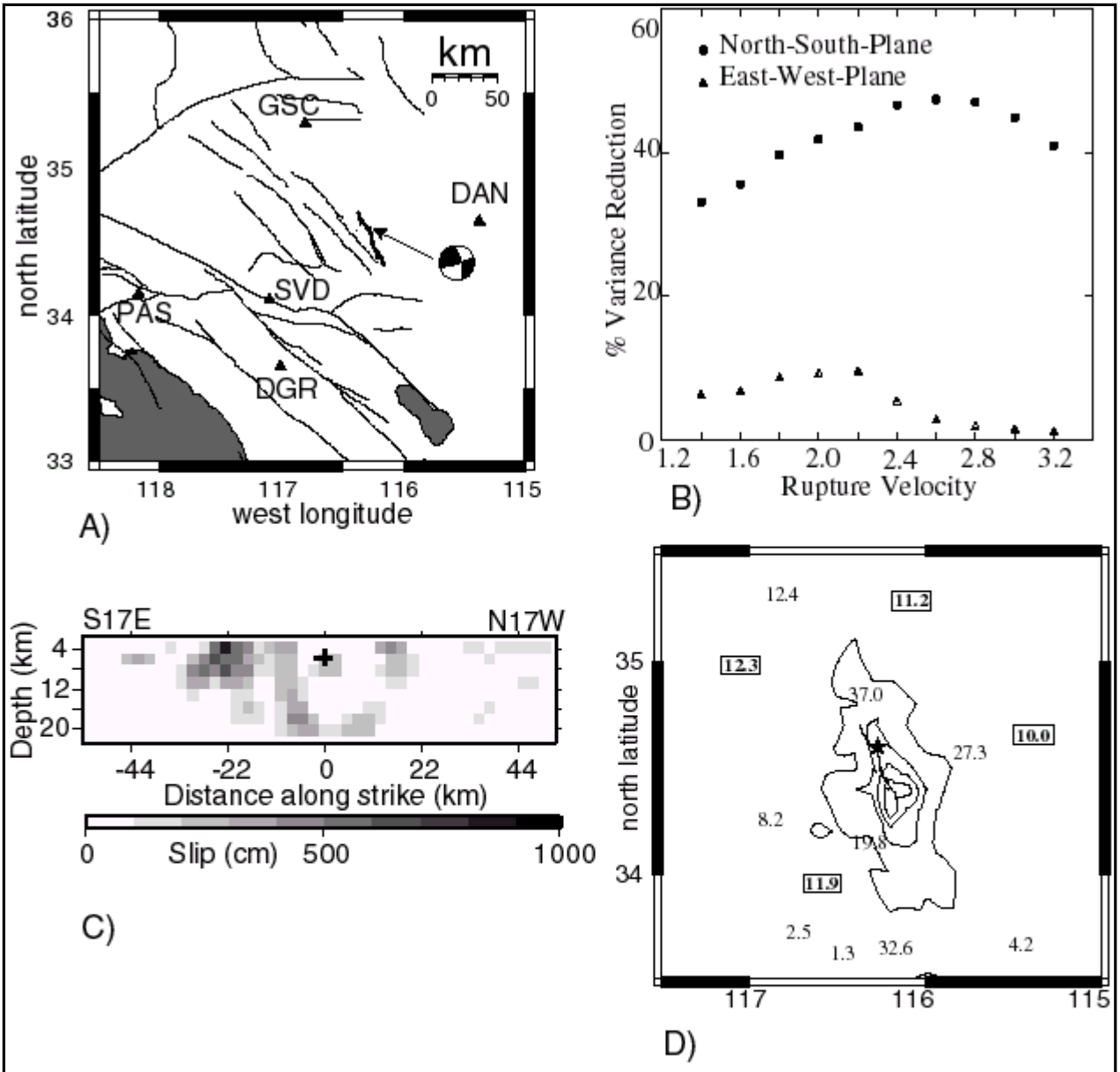

Figure 2.3. A) Location map showing stations used to invert for slip distribution (triangles), and seismic moment tensor. The arrow points to the epicenteral location. B) The variance reduction is plotted against the rupture velocity for the two possible nodal planes. C) The slip distribution for the north-northwest striking nodal plane. The hypocenter is indicated by the plus symbol. D) Simulated near-fault ground motions (contours at 20 cm/s intervals) are compared to observations (numerical values in cm/s). Only the values enclosed in boxes were available in the realtime epoch.

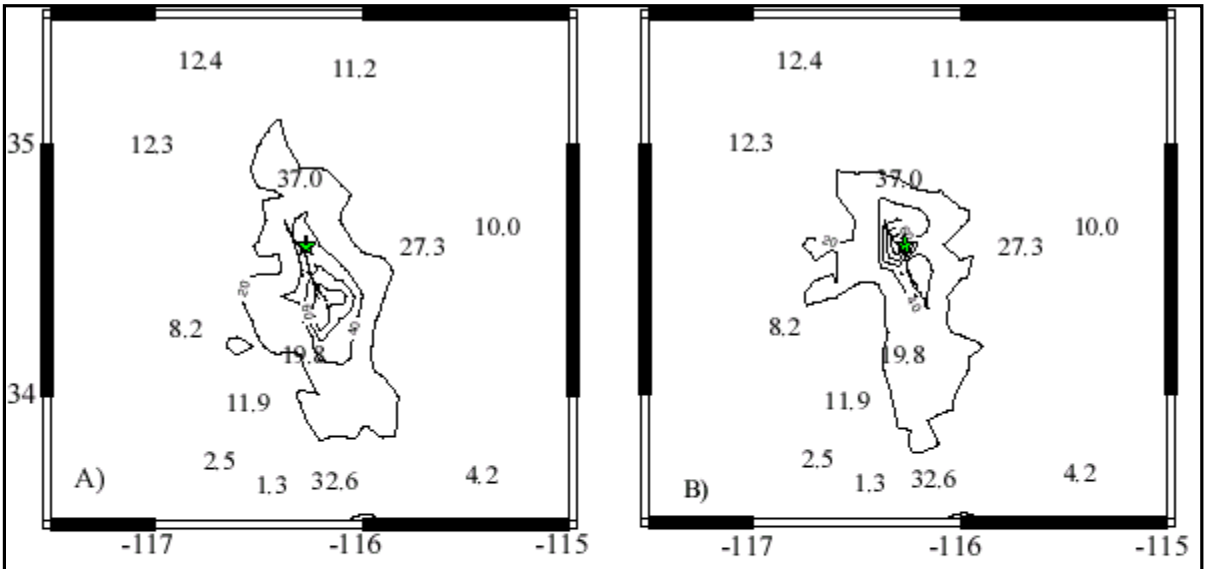

Figure 2.4. A) Comparison of simulated and observed PGV as shown in Figure 2.3b. B) Comparison of simulated and observed PGV using the more complex kinematic faulting model of Kaverina et al. [2002] (provided in the appendix). Note that the maximum PGV and the area with greater than 20 cm/s PGV are similar in the two plots, but that the very near-fault details differ. It is also interesting to note that the more complex model retains a component of southward directivity, which is expressed through the elongation of the 20 cm/s contour.

Given what we now know about the considerable spatial and temporal complexity of the Hector Mine earthquake it is instructive to simulate the near-fault strong ground motions to compare with the results of the earlier study. Figure 2.4 compares the peak horizontal ground velocity (PGV) map in Dreger and Kaverina [2000] with a PGV map derived from the combined inversion results of Kaverina et al. [2002]. The two simulations yield a comparable level of near-fault PGV. Both PGV models correlate well with the peak value observed at station HEC (37 cm/s; Figure 8), and also the station that registered 19.8 cm/s. Both models tend to under-predict the large values to the east (27.3 cm/s) and to the south (32.6 cm/s). These misfits are likely due to unaccounted for site amplification, or basin structure. Although the PGV maps differ in the near-fault details, the overall area that apparently experienced greater than 20 cm/s PGV is similar in the two simulations indicating that the preliminary map (Figure 2.4A), if rapidly determined, would have value in emergency response applications.

3. Analysis Review Tool

In parallel with the development of the automated finite-fault procedures and the integration of the ShakeMap software, we have developed a Web-based analysis tool for reviewing results. Because of the complicated nature of the finite-fault and ShakeMap software, this tool is critical to allow an analyst to interact with the automated results, make changes and rerun programs. The interface allows the user to select/deselect stations, modify the location and fault plane parameters, and to adjust weighting and other inversion controls. It is designed to be integrated with the ShakeMap software, so the reviewed results can be used to generated an updated map. Figure 3.1 illustrates the analyst interface as it was applied to the 08/10/2001 Portola earthquake.

On August 10, 2001 at 20:19:26UTC a 5.5 event occurred 15 km west of Portola, California (39.893, -120.638). This event was processed by the automatic system and a seismic moment tensor was obtained within 8 minutes, indicating a strike-slip mechanism (strike=328., rake=-170., dip=84) with scalar seismic moment of 4.39e+23 dyne cm. This is a small event, and not expected to deviate significantly from a point-source. As expected for such a small event, the finite-fault results were marginal. The line source inversions yielded a rupture velocity of 1 km/s, the lowest allowed. The low value reflects the desire of the code to attempt to map slip close to the hypocenter. Although the line source results indicated a slight preference for the NW trending plane, the difference was so slight that both planes were tested during the full 2D plane inversion. The plane source inversion results evaluated using a variance reduction measure of goodness of fit of 10.9% for the SW-trending plane and 10.4% for the NW trending plane demonstrate the difficulty of obtaining finite-source information for small events.

The inversion results were reviewed using the Analyst Interface. A number of iterations were made investigating different combinations of stations, fault dimensions, and values of dislocation rise time and rupture velocity. Based on historical seismicity in the region, the NW plane was assumed to be the actual plane. Reasonably good results were found using 6 three-component stations (CMB, KCC, MOD, ORV, WDC, YBH) located in the 180-300 km distance range from the source. Figure 3.2a shows the seismic moment tensor solution for the event and the

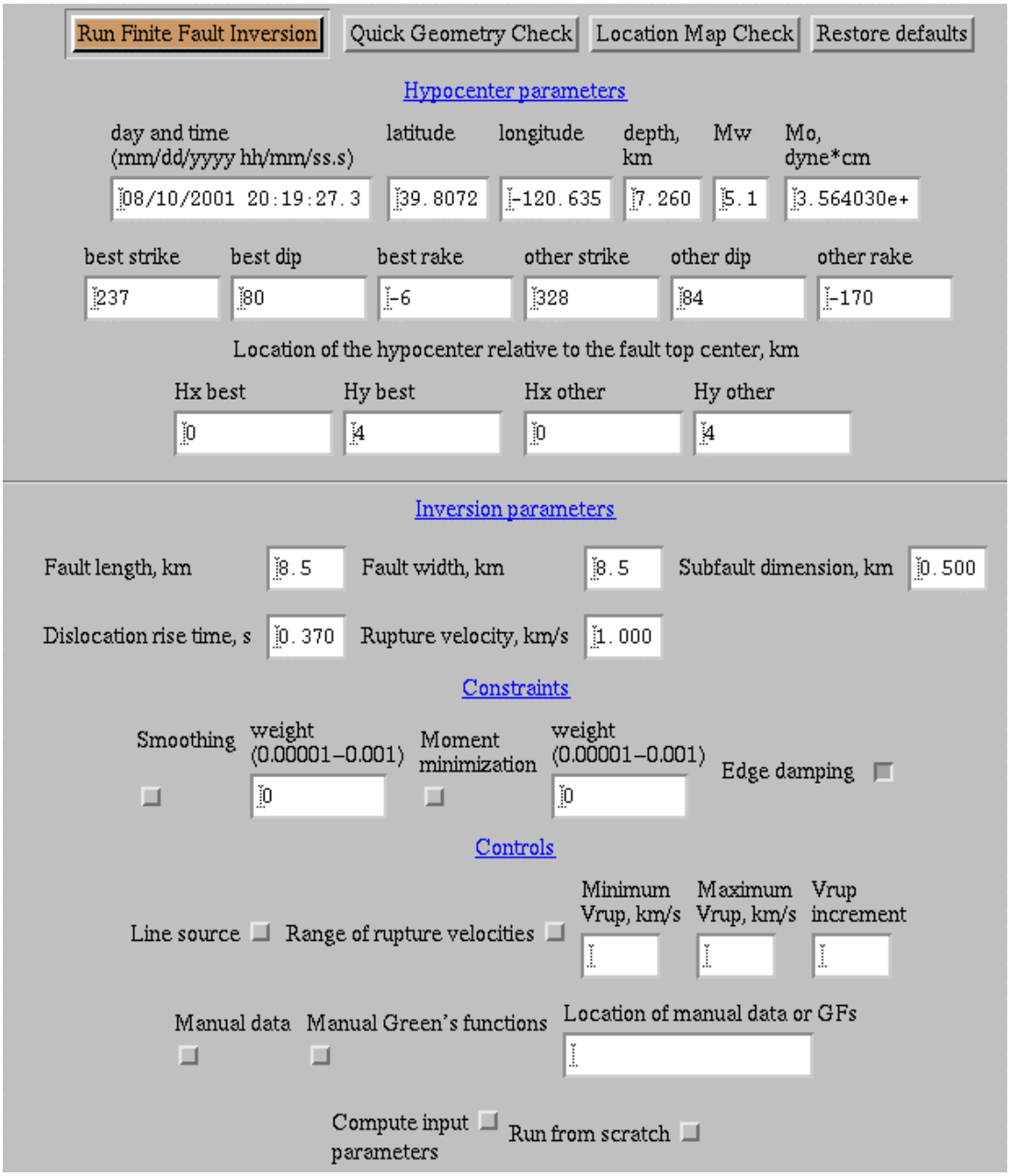

Figure 3.1 Illustration of the analyst interface developed to facilitate the review of the finite-fault and ShakeMap results.

locations of stations used in the inversion. Figure 3.2b shows the slip distribution for the NW striking plane, which was found to locate close to the hypocenter when a 0.5s delay was applied to the Green's functions. The delay is necessary to account for possible errors in event origin time. The rupture velocity was set to a more realistic value of 2 km/s. The variance reduction for the NW and SW striking planes were 20 and 25%, respectively. Both fit considerably better than the automatic result. The scalar seismic moment from the reviewed inversion is 2.46e+23 dyne

cm corresponding to Mw4.9. Figure 3.2c and 3.2d compare the peak ground acceleration TriNet ShakeMap and the Conservative ShakeMap. The two maps are very similar in terms of the extent

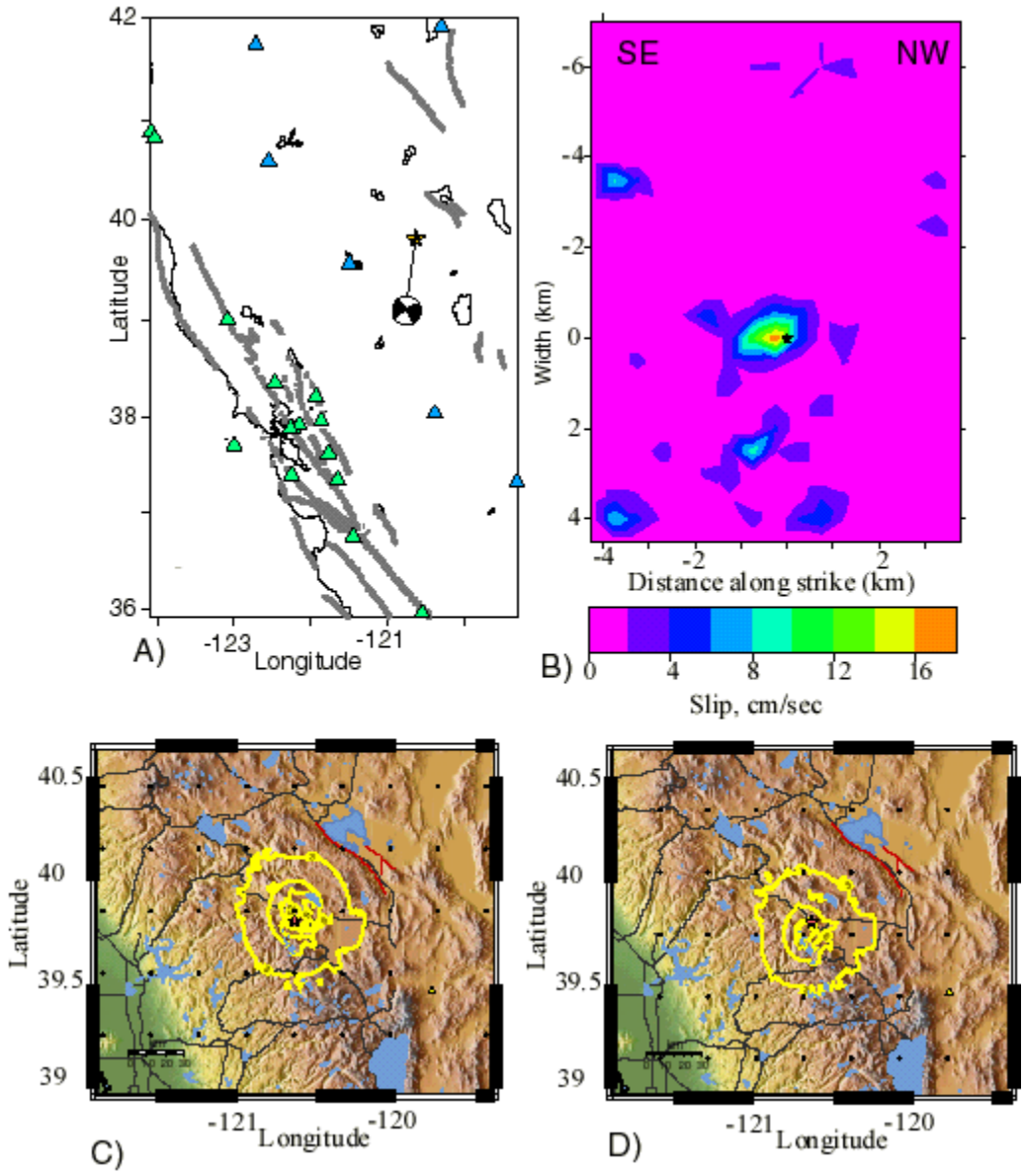

Figure 3.2. Illustration of the finite-fault results from the August 10, 2001 Portola earthquake. A) Map showing the location and mechanism, and stations used in the finite-fault inversion (blue triangles). B) Distribution of slip on the northwest trending plane. C) TriNet ShakeMap, and D) Conservative ShakeMap results for PGA. The contours are for intervals of 3% g.

of the strong shaking, and peak values, however the location of the peak is offset in the Conservative ShakeMap due to the contribution from the finite-fault results.

4. Conclusions

4.1 Summary of Work Completed

The finite-fault/ShakeMap packages developed under this contract were implemented in the REDI system in April of 2001. This package includes the finite-source inverse code, managing software for realtime processing control and exchange information with ShakeMap V2.x. An email information exchange format has been developed for interested parties such as PG&E and the U.S. Geological Survey. All components of the package were screened for bugs and improved for robust realtime processing. The system is configured so that any event of M 4.9 and greater will trigger the finite-fault processing system in order to test the software. The largest event that has occurred since the implementation was an earthquake in the Portola area of the Sierra Nevada. Although only a moderate event, it provides an example of the implementation as well as the newly developed Analyst Interface. The Portola test case indicated that all of the components function properly.

All of the examples of the ShakeMaps in this report (Hector Mine, Mammoth Lakes and Portola) illustrate the importance of this methodology in areas of limited station coverage, where the estimated near-fault ground motions may be the only available information.

4.2 Future Activities

The Berkeley group is working with the U.S. Geological Survey ShakeMap working groups in Menlo Park and Pasadena toward implementation of the finite-source component into the authoritative ShakeMap system for California. Additionally, the Berkeley group continues to monitor the realtime implementation of the software package, perform testing, and apply software updates. The BSL seismic alarm response team is also providing a continued review of finite-source and ShakeMap results produced by the system, and will communicate the results to the U.S. Geological Survey ShakeMap group in the event of triggering earthquakes.

5. References

Dreger, D. S. and A. Kaverina (2000). Seismic remote sensing for the earthquake source process and near-source strong shaking: a case study of the October 16, 1999 Hector Mine earthquake, *Geophys. Res. Lett.,* 27, 1941-1944.

Ji, C., D. J. Wald, and D. V. Helmberger (2002). Source description of the 1999 Hector Mine, California earthquake. Part II: Complexity of slip history, *Bull. Seism. Soc. Am. Special Issue*.

Kaverina, A., D. Dreger, and E. Price (2002). The combined inversion of seismic and geodetic data for the source process of the 16 October, 1999, Mw7.1 Hector Mine, California, earthquake, *Bull. Seism. Soc. Am. Special Issue*.

Hartzell, S. H., and T. H. Heaton (1983). Inversion of strong ground motion and teleseismic waveform data for the fault rupture history of the 1979 Imperial Valley, California, earthquake, *Bull. Seism. Soc. Am.,* 73, 1553-1583.

Pasyanos, M. E., D. S. Dreger, and B. Romanowicz (1996). Toward real-time estimation of regional moment tensors, *Bull. Seism. Soc. Am*., 86, 1255-1269.

Somerville, P.G., N.F. Smith, R.W. Graves, and N.A. Abrahamson (1997). Modification of empirical strong ground motion attenuation relations to include the amplitude and duration effects of rupture directivity, *Seism. Res. Lett*., 68, 199-222.

Somerville, P. G., K. Irikura, R. Graves, S. Sawada, D. Wald, N. Abrahamson, Y. Iwasaki, T. Kagawa, N. Smith, and A. Kowada (1999). Characterizing crustal earthquake slip models for the prediction of strong ground motion, Seism. Res. Lett., 70, 59-80.

Wald, D. J., V. Quitoriano, T. H. Heaton, H. Kanamori, C. W. Scrivner, and C. B. Worden (1999) TriNet ``ShakeMaps'': Rapid Generation of Instrumental Ground Motion and Intensity Maps for Earthquakes in Southern California, *Earthquake Spectra,* 15, 537-555.

Wells, D. L., and K. J. Coppersmith (1994). New empirical relationships among magnitude, rupture length, rupture width, rupture area, and surface displacement, *Bull. Seism. Soc. Am*., 84, 974-1002, 1994.

Wessel, P., and W. H. F. Smith (1991). Free software helps map and display data, EOS, 445-446.

6. Appendix

6.1 Geophysical Research Letters paper on the application of this method for the 1999 Hector Mine, California earthquake.

6.2 Bulletin of the Seismological Society of America paper on the detailed analysis of the source process of the 1999 Hector Mine, California earthquake.